Quantitative VOI-based Analysis of Template-guided Attenuation Correction in 3D Brain PET

Marie-Louise Montandon and Habib Zaidi, *Senior Member, IEEE*

***Abstract*— A transmission template-guided attenuation correction method was recently proposed and validated in comparison to transmission-based attenuation correction using voxelwise SPM analysis of clinical data. In contrast to brain activation studies, brain PET research studies often involve absolute quantification. As the assessment was carried out by a SPM group analysis alone, validation as to how such quantification can be affected by the two methods needed to be performed to demonstrate how the proposed method performs individually, particularly for diagnostic applications or individual quantification. In this study, we assess the quantitative accuracy of this method using automated volume of interest (VOI)-based analysis by means of the BRASS software for automatic fitting and quantification of functional brain images. There is a very good correlation (R^2=0.91) between the Atlas-guided and measured transmission-guided attenuation correction techniques and the regression line agreed well with the line of identity (slope=0.96). The mean absolute relative difference between the two methods for all VOIs across the whole population is 2.3% whereas the maximum difference is less than 7%. No proof of statistically significant differences could be verified for all regions. These encouraging results provide further confidence in the adequacy of the proposed approach demonstrating its performance particularly for research studies or diagnostic applications involving quantification.**

I. Introduction

Among the many challenges facing quantitative brain PET, it is well accepted that photon attenuation in tissues is the primary physical degrading factor limiting both visual qualitative interpretation and quantitative analysis capabilities of reconstructed PET images [1]. Measured transmission-based attenuation correction in cerebral 3D PET imaging is the most common used procedure both in clinical and research settings since it is expected to yield the best attenuation map as a result of matched energy and spatial resolution. However, motion-induced misalignment between transmission (TX) and emission (EM) scans can result in erroneous estimation of regional tissue activity concentrations. Likewise, the high cost of combined PET/CT units and the potential introduction of artefacts in the presence of metallic dental implants when using CT-based attenuation correction (AC), thus biasing quantitative PET estimates and disturbing the visual interpretation of PET images, are major limitations for brain imaging dedicated facilities [2]. The search for reduction of acquisition time in brain PET scanning protocols spurred the development of transmissionless algorithms for derivation of the non-uniform attenuation map, thus eliminating the need for acquisition of a measured TX scan. More recently, we investigated the implementation and applicability of Atlas-guided AC [3]. Twelve cerebral clinical studies were used for evaluation of the developed AC technique as compared to the standard pre-injection measured TX-based method used in clinical routine (gold standard). The subjective qualitative assessment showed no significant visual differences between Atlas-guided and TX-based AC methods. However, the quantitative voxel-based analysis using Statistical Parametric Mapping (SPM2) [4] comparing Atlas-guided to TX-based ACs suggested that regional brain metabolic activity increases significantly bilaterally in the superior frontal and precentral gyri, in addition to the left middle temporal gyrus and the left frontal lobe. Conversely, activity decreases in the corpus callosum in the left parasagittal region.

It was hypothesized that the overall diagnostic accuracy may not be too influenced by the two correction methods for certain diseases such as dementia of Alzheimer's type (DAT), but regional quantitative accuracy is most likely affected. If regional discrepancies are not anatomically consistent (i.e., differences in regional attenuation between Atlas estimates and actual individual brains), the SPM group validation alone is not sufficient to depict effects and limitations of the proposed AC method. It is quite important to demonstrate how the proposed method performs individually, particularly for diagnostic applications or individual quantification. In this study, we further assess the quantitative accuracy of this method in clinical setting using volume of interest (VOIs)-based analysis by means of the commercially available *BRASS* program for automatic fitting and quantification of functional brain images [5].

II. Materials and Methods

A. Atlas-guided Attenuation Correction

The developed algorithm derives patient-specific attenuation map by anatomic standardization through nonlinear warping of a stereotactic TX template obtained by averaging 11 scans of normal subjects [3]. This TX template is coregistered to a specially designed tracer-specific ^{18}F-[FDG] EM template constructed by scanning 17 normal subjects in resting condition during tracer uptake in a dark room [6]. The EM template is first coregistered and spatially normalized to

This work was supported by the Swiss National Science Foundation under grant SNSF 3152A0-102143.

Marie-Louise Montandon (e-mail: marie-louise.montandon@hcuge.ch) and Habib Zaidi (e-mail: habib.zaidi@hcuge.ch) are with the Division of Nuclear Medicine, Geneva University Hospital, CH-1211 Geneva, Switzerland

preliminary PET images of subjects corrected for scatter and attenuation using an approximate method since this has been shown to improve registration accuracy. The preliminary 3-D PET reconstructions relied on calculated AC, which was performed by approximating the outline of the head on each transverse slice using a manually drawn slice-dependent ellipse assuming uniform attenuation (μ=0.096 cm^{-1}) for brain tissues [7]. The resulting transformation matrices are recorded and re-applied to the TX template. The attenuation of the rigid bed was neglected. The derived attenuation map is then forward projected to generate AC factors to be used for correcting the subjects' PET data. Fig. 1 shows a diagram describing the general principles of the method and main steps required to generate a patient-specific attenuation map.

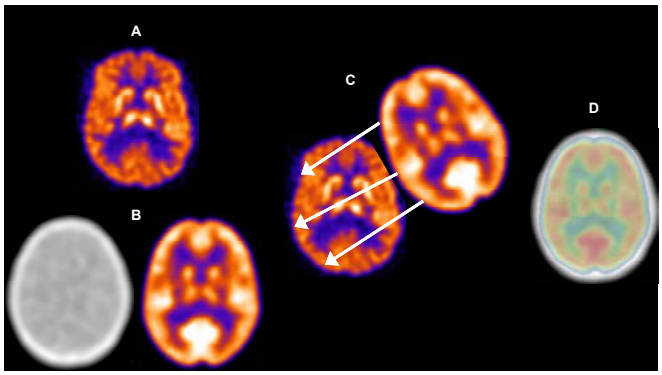

Fig. 1. Illustration of the principle of Atlas-guided derivation of the attenuation map. (**A**) Preliminary PET reconstruction obtained using calculated AC. (**B**) ^{18}F-[FDG] EM and TX templates used in this study. (**C**) EM template is spatially normalized to preliminary PET reconstruction. (**D**) Application of same transformation to TX template.

B. PET Data Acquisition and Reconstruction

The study population consisted of 9 women in the early stage of DAT. Their age ranged from 68 to 81 years (mean±SD=75.44±5.0). The 9 subjects were drawn randomly from a large pool of DAT patients participating in a study focusing on the neurofunctional effects of donepezil, a cholinesterase inhibitor, which is a medication used in the treatment of mild to moderate dementia of Alzheimer's type. This study was approved by the ethical committee of Geneva University Hospital and the Swiss Federal radiation protection authorities. All patients gave their written informed consent for participation in the study protocol.

The method used in clinical routine in our department for AC is based on the acquisition of an additional pre-injection TX scan (10 minutes) using ^{137}Cs single-photon sources. A thermoplastic face mask was used to limit head motion and for accurate repositioning of patients for the EM scan. PET data acquisition (25 min) started 30 min after intravenous injection of approximately 222 MBq of ^{18}F-[FDG] on the ECAT ART continuously rotating partial-ring positron tomograph (CTI/Siemens, Knoxville, TN) operated in fully 3-D mode. Images were reconstructed using analytic 3DRP reprojection algorithm [8] with a maximum acceptance angle corresponding to 17 rings and a span of 7. The default parameters used in clinical routine were applied (Ramp filter, cut-off frequency 0.35 cycles/pixel). The reconstructed images consist of 47 slices with 128x128 resolution and a voxel size set to 1.72 *x* 1.72 *x* 3.4 mm^3.

Scatter correction was performed using a model-based scatter correction algorithm which combines both the EM scan and attenuation map together with the physics of Compton scattering to estimate the scatter distribution [9]. The Atlas-guided AC matrix is calculated by forward projection at appropriate angles of the resulting attenuation map. The generated AC factors are then used to correct the EM data. Therefore, the Atlas-guided attenuation map served for both scatter and AC purposes.

C. Quantitative Image Analysis Using BRASS

The images reconstructed with measured AC served as gold standard for assessment of the newly developed Atlas-guided attenuation compensation. Reconstructed PET images using both AC methods were analysed using the *BRASS* commercial automated functional brain analysis software (Hermes *BRASS* software, Nuclear Diagnostics AB, Sweden). Briefly, *BRASS* fits and compares patient images to 3-D reference templates created from images of healthy subjects. The TX and Atlas-guided reconstructed PET images were registered individually to the BRASS template for quantitative analysis. The ^{18}F-[FDG] template used in this work was built by averaging 12 PET images of normal subjects acquired on an ECAT EXACT HR$^+$ PET scanner (Siemens/CTI, Knoxville TN) in a fasting state with eyes open, ears plugged, and in a moderately lit environment. Fig. 2 illustrates transverse, coronal and sagittal views of the 3-D anatomically standardised brain template and the region map consisting of a total of 63 regions defined on this template for automated VOI quantification [5].

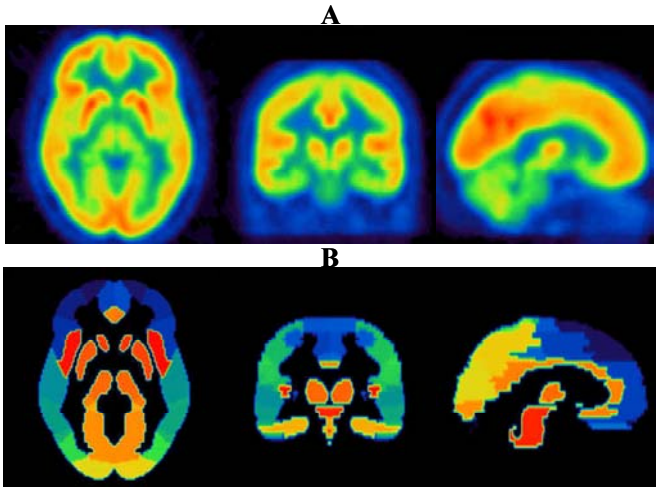

Fig. 2. Transverse, coronal and sagittal views (left to right) of the 3-D anatomically standardized brain template (**A**) and the region map consisting of 63 VOI regions in total defined on this template for automated VOI quantification (Hermes *BRASS* software, Nuclear Diagnostics AB, Sweden).

The correlation between mean activity concentration estimates obtained when using the two AC methods was checked on a VOI by VOI basis and using pooled VOI analysis. The means, standard errors and standard deviations of activity concentration estimates from clinical PET images reconstructed using both protocols were compared. The relative difference was used as a figure of merit for comparative assessment both within subject and as group consisting of a homogenous population. It is defined as:

$$Percent\ difference = \frac{VOI(Atlas-guided) - VOI(TX-guided)}{VOI(TX-guided)} \times 100\%$$

Statistical analysis was performed VOI by VOI using repeated ANOVA to assess the significance of the differences between mean activity concentration estimates in patient studies when using the Atlas-guided as compared to the TX-guided reconstructions (significant P value<0.05). It should be noted that failure to prove statistically significant differences is not sufficient to confirm that the results are statistically identical.

III. Results

Typical patient brain non-uniform attenuation maps and corresponding PET images acquired on the ECAT ART camera and reconstructed with measured TX as well as Atlas-guided AC are shown in Fig. 3. The qualitative subjective assessment performed by expert physicians showed no significant visual differences between Atlas-guided and TX-based reconstruction methods [3]. Fig. 4 illustrates the means, standard errors as well as standard deviations of the relative differences between the two correction methods resulting from the quantitative analysis for the 63 VOIs, for each of the 9 patients studied. The relative difference between the two methods for all VOIs within subject is less than 9%. Fig. 5 shows a linear regression plot illustrating correlation between the two AC algorithms for both a single patient having an average slope of 0.94 (R^2=0.87) and grouped analysis comprising the 9 patients involved in the study. The line connecting the data points represents the result of a linear regression analysis.

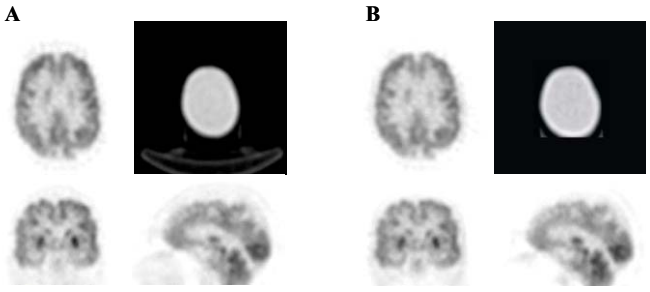

Fig. 3. Filtered backprojection reconstructions of clinical 3-D brain PET images presented in different planes together with a corresponding slice of the attenuation map comparing measured (**A**) and Atlas-guided (**B**) AC techniques.

Table 1 summarizes the regression analysis results of the patient data including the slopes, intercepts and correlation coefficients. There is a very good correlation (R^2=0.91) between the Atlas-guided and measured TX-guided AC techniques and the regression line agreed well with the line of identity (slope=0.96) for the grouped analysis. The dispersion of data points is insignificant and the general trend as shown by the regression line is that the coefficients of variations are similar. However, Atlas-guided AC leads to higher overall estimates than measured AC. This would appear to result from a difference between the attenuation coefficient values in both methods and thus the AC factors applied. According to these results, the attenuation coefficients derived from the template obtained by positron-emitting ^{68}Ga/^{68}Ge rod sources appear to be slightly higher overall than estimates obtained from actual measured data using single-photon ^{137}Cs point sources. Moreover, our analysis suggests that the intercept in the regression line is significantly different from zero.

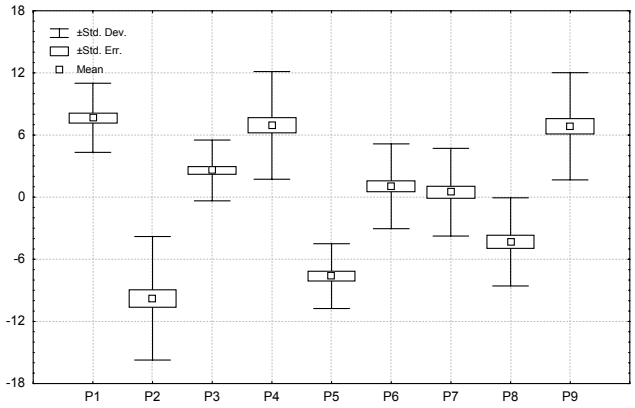

Fig. 4. Box & Whisker plots showing relative differences between reconstructions obtained by performing AC guided by measured TX and normalized standardized TX template. Means, standard errors as well as standard deviations are calculated for each of the 9 patients studied.

The statistical comparison between activity concentration estimates when using the two AC techniques showed that the correlation for all VOIs and all patients is high. The percent differences between the two AC techniques are minor and no proof of statistically significant differences ("the two distributions are not the same") could be verified for all regions. Fig. 6 shows the means, standard errors as well as standard deviations of the relative difference between absolute activity concentration estimates for clinical brain 3-D reconstructions using AC guided by measured TX and 3-D reconstructions guided by standardized TX template in each of the 63 VOIs, averaged across the 9 patients studied. It can be seen that the maximum difference between the individual values is less than 8%. Likewise, the mean absolute relative difference between the two methods for all VOIs across the whole population (differences of the population means) is 2.3% whereas the maximum difference is less than 7%. These results seem to suggest a 10% anterior-posterior gradient for a grouped data analysis performed by grouping the VOIs into regions by spatial location (i.e., medial/lateral, anterior/posterior, superior/inferior).

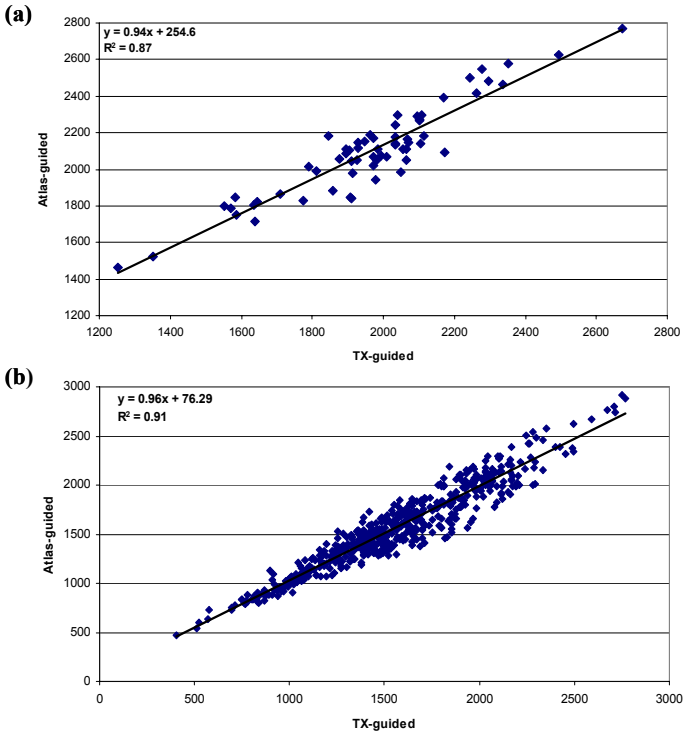

Fig. 5. Correlation plots between clinical 3-D brain scans reconstructed using AC guided by measured TX (abscissa) and 3-D reconstructions guided by normalized standardized template (ordinate). Sixty three data points for a single patient (**a**) and 567 data points representing mean values of the 63 VOIs resulting from the analysis of the 9 patients studied are shown (**b**) together with best fit equations and correlation coefficients.

IV. Discussion

Despite the progress made in quantitative imaging, physical factors still degrade the actual image and thus the true activity obtained by PET measurements in functional brain imaging [10]. Therefore, it is not surprising that to improve brain mapping, it is imperative to investigate the impact of correction techniques for physical degradation factors such as attenuation, scatter and resolution loss or partial volume effect. Several methods have been devised to correct for attenuation in neurological PET studies that do no require an always noisy transmission scan [3, 11-14]. It is worth emphasizing that despite the worthwhile research that has been performed in this area, there is no clear evidence that current commercial products allow applicability of these techniques in a clinical environment [1].

Evaluation and clinical validation of image correction and reconstruction algorithms is inherently difficult and sometimes unconvincing. There is a clear need for guidelines to evaluate quantitative techniques and other image processing issues in PET. Voxel-based or VOI-based analysis of PET algorithmic designs is intrinsically based on a large number of variables which all affect the final result to a greater or lesser extent. Acquisition and reconstruction options rely on isotope, acquisition time/injected activity, randoms, scatter and attenuation correction, reconstruction algorithm, pre- and/or post-filtering, …etc. Subsequent analysis is done after (intra-individual) coregistration, anatomical standardization (spatial normalization) and smoothing. Therefore, it is clear that a multi-parameter optimization procedure is necessary to determine the optimal conditions for measuring defects or activations [15]. The clinical relevance of small but systematic differences (<8%) between the two attenuation correction methods is hard to predict and will depend on the diagnostic paradigm followed by clinicians to interpret brain PET data. Current procedures for interpreting clinical data in many PET facilities are still based on mere visual assessment. It has been shown that different attenuation correction techniques have little effect on subjective visual interpretation of brain PET images [14].

TABLE I
SUMMARY OF REGRESSION ANALYSIS RESULTS REPORTING SLOPES, INTERCEPTS AND REGRESSION COEFFICIENTS FOR THE 9 PATIENTS INCLUDED IN THIS STUDY.

	slope	intercept	R^2
Patient 1	1.00	123.94	0.93
Patient 2	0.80	177.31	0.84
Patient 3	1.01	24.83	0.96
Patient 4	0.94	254.60	0.87
Patient 5	0.82	159.02	0.90
Patient 6	0.93	86.68	0.96
Patient 7	1.06	115.82	0.96
Patient 8	0.90	131.79	0.83
Patient 9	1.00	89.83	0.89

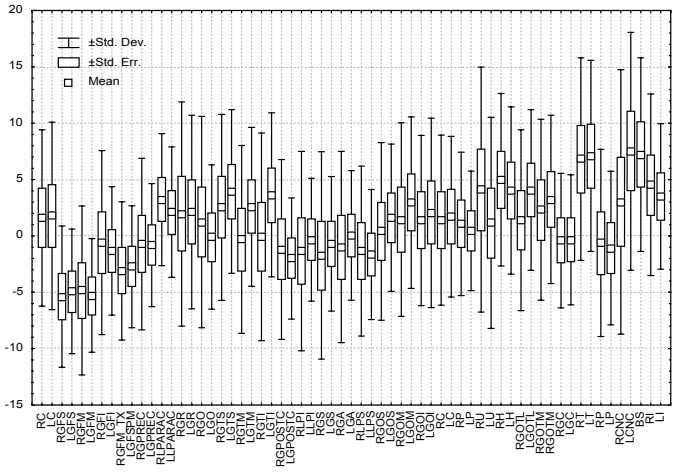

Fig. 6. Box & Whisker plots showing relative differences for the 63 VOIs between absolute activity concentration estimates for clinical brain 3-D reconstructions using AC guided by measured TX and 3-D reconstructions guided by normalized standardized TX template. Means, standard errors as well as standard deviations are calculated across the 9 patients studied.

The Atlas-guided technique will tend to scale the skull size based on the brain size. Our experience with the limited set of clinical data used for validating the algorithm suggests that there is small variability in brain sizes for the homogeneous population studied as large brains were not encountered. An in-depth discussion of relevant issues including the effect of abnormal anatomy and/or uptake in patients as well as the relevance of building tracer-specific templates especially for PET radioligands to allow application of the proposed algorithm for children and other tracers are given in [3]. For

the former, the use of cost-function masking to exclude abnormal anatomy or uptake is envisaged to avoid biasing the transformations computed by the normalization procedure.

Nowadays, manual ROI analyses are no longer of much clinical interest since a long time is required to draw accurately the ROIs needed to cover an entire brain and the operator-dependent variability is large compared to inter-individual physiological variability. The artificial boundaries from the ROI or VOI region map and the relatively large search volumes constitute a known inherent disadvantage of VOI techniques in the sense that they imply a preconception about the topography of the functional deficits and that the size of the VOI imposes a spatially smoothing effect [16]. Smaller focal defects can be observed by the voxel-based techniques and a brain region can be reported as abnormal even when only part of the underlying VOI was hypoperfused (dilution effect). Additional tools for subject-to-group statistical comparisons should be available with automatic VOI software and these should take into account the special problems of correction for multiple comparisons [17, 18]. However, if sufficient variance from the VOI measurements is included, the overall performance of automated stereotactic VOI-based analysis can be similar to that of the voxel-based analysis for the same discrimination task. In some studies, VOI-based analysis performed poorly at low false-positive fraction and was less tolerant to noise than the voxel-based analysis [19]. Another study found that under clinical conditions (in traumatic brain injury and cognitive impairment), classification of brain SPECT studies can greatly be aided by anatomic standardization techniques and that under the investigated circumstances, SPM was found to have a lower sensitivity than VOI or voxelwise region-growing techniques, at low false-positive fractions, in contrast to the former study [20]. Among the commercial packages, *BRASS* is specifically oriented towards routine clinical brain SPECT and PET applications, and allows voxel-wise comparison of individual studies by means of statistical intensity differences, compared to a mean and standard deviation image from a control group, based upon region-growing of deviating voxels.

V. Conclusion

A recently developed new Atlas-guided non-uniform attenuation correction method for 3-D brain PET imaging was assessed quantitatively using clinical studies and automated functional brain analysis software as an adjunct to the voxel-based analysis performed previously. The algorithm is unsupervised and shows a comparable image quality with significant reduction in overall patient scanning time duration and radiation absorbed dose. These encouraging results provide further confidence in the adequacy of the proposed method demonstrating its performance particularly for diagnostic applications involving quantification.

References

[1] H. Zaidi, M-L. Montandon and S. R. Meikle, "Strategies for attenuation compensation in neurological PET studies," *NeuroImage*, 2007 *in press*

[2] E. M. Kamel, C. Burger, A. Buck, G. K. von Schulthess, and G. W. Goerres, "Impact of metallic dental implants on CT-based attenuation correction in a combined PET/CT scanner," *Eur Radiol*, vol. 13, pp. 724-8, 2003.

[3] M.-L. Montandon and H. Zaidi, "Atlas-guided non-uniform attenuation correction in cerebral 3D PET imaging.," *Neuroimage*, vol. 25, pp. 278-286, 2005.

[4] K. Friston, J. Ashburner, J. Heather, A. Holmes, and J. B. Poline, "Statistical Parametric Mapping (SPM2)," The Wellcome Department of Cognitive Neurology, University College London, London Available at www.fil.ion.ucl.ac.uk/spm, 2003.

[5] P. J. Slomka, P. Radau, G. A. Hurwitz, and D. Dey, "Automated three-dimensional quantification of myocardial perfusion and brain SPECT.," *Comput Med Imaging Graph*, vol. 25, pp. 153-164, 2001.

[6] J. D. Gispert, J. Pascau, S. Reig, R. Martinez-Lázaro, V. Molina, and M. Desco, "Influence of the normalization template on the outcome of statistical parametric mapping of PET scans.," *NeuroImage*, vol. 18, pp. 601-612, 2003.

[7] H. Zaidi, M.-L. Montandon, and D. O. Slosman, "Attenuation compensation in cerebral 3D PET: effect of the attenuation map on absolute and relative quantitation.," *J Nucl Med*, vol. *submitted*, 2003.

[8] P. E. Kinahan and J. G. Rogers, "Analytic 3D image reconstruction using all detected events.," *IEEE Trans Nucl Sci*, vol. 36, pp. 964-968, 1989.

[9] C. C. Watson, "New, faster, image-based scatter correction for 3D PET.," *IEEE Trans Nucl Sci*, vol. 47, pp. 1587-1594, 2000.

[10] H. Zaidi and V. Sossi, "Correction for image degrading factors is essential for accurate quantification of brain function using PET.," *Med Phys*, vol. 31, pp. 423-426, 2004.

[11] S. Siegel and M. Dahlbom, "Implementation and evaluation of a calculated attenuation correction for PET.," *IEEE Trans Nucl Sci*, vol. 39, pp. 1117 -1121, 1992.

[12] B. T. Weinzapfel and G. D. Hutchins, "Automated PET attenuation correction model for functional brain imaging.," *J Nucl Med*, vol. 42, pp. 483-491, 2001.

[13] H. Zaidi, M.-L. Montandon, and D. O. Slosman, "Magnetic resonance imaging-guided attenuation and scatter corrections in three-dimensional brain positron emission tomography.," *Med Phys*, vol. 30, pp. 937-948, 2003.

[14] H. Zaidi, M.-L. Montandon, and D. O. Slosman, "Attenuation compensation in cerebral 3D PET: effect of the attenuation map on absolute and relative quantitation.," *Eur J Nucl Med Mol Imaging*, vol. 31, pp. 52-63, 2004.

[15] J. M. Links, "Special issues in quantitation of brain receptors and related markers by emission computed tomography.," *Q J Nucl Med*, vol. 42, pp. 158-165, 1998.

[16] P. D. Acton and K. J. Friston, "Statistical parametric mapping in functional neuroimaging: beyond PET and fMRI activation studies.," *Eur J Nucl Med*, vol. 25, pp. 663-667, 1998.

[17] M. Signorini, E. Paulesu, K. Friston, D. Perani, A. Colleluori, G. Lucignani, F. Grassi, V. Bettinardi, R. S. Frackowiak, and F. Fazio, "Rapid assessment of regional cerebral metabolic abnormalities in single subjects with quantitative and nonquantitative [18F]FDG PET: A clinical validation of statistical parametric mapping.," *Neuroimage*, vol. 9, pp. 63-80, 1999.

[18] R. A. Weeks, V. J. Cunningham, P. Piccini, S. Waters, A. E. Harding, and D. J. Brooks, "11C-diprenorphine binding in Huntington's disease: a comparison of region of interest analysis with statistical parametric mapping," *J Cereb Blood Flow Metab*, vol. 17, pp. 943-949, 1997.

[19] J. S. Liow, K. Rehm, S. C. Strother, J. R. Anderson, N. Morch, L. K. Hansen, K. A. Schaper, and D. A. Rottenberg, "Comparison of voxel- and volume-of-interest-based analyses in FDG PET scans of HIV positive and healthy individuals," *J Nucl Med*, vol. 41, pp. 612-621, 2000.

[20] K. J. Van Laere, J. Warwick, J. Versijpt, I. Goethals, K. Audenaert, B. van Heerden, and R. Dierckx, "Analysis of clinical brain SPECT data based on anatomic standardization and reference to normal data: an ROC-based comparison of visual, semiquantitative, and voxel-based methods," *J Nucl Med*, vol. 43, pp. 458-469, 2002.